# Optimization and Fiber-Centered Prediction of Functional Network ROIs

Can Feng[1], Tianming Liu[2], Liang Xiao[1], and Zhihui Wei[1]

[1] School of Computer Scicence, Nanjing Unieversity of Science & Technology
210094 Nan Jing, China
[2] Department of Computer Science, The University of Georgia,
30605, Athens, GA, USA

**Abstract.** Study of functional and structural brain networks via fMRI and DTI data has received significant interest recently. A fundamental and challenging problem to identify a specific brain networks is how to localize the best possible regions of interests (ROIs). In this paper, we firstly propose a new approach to quantitatively describe fiber bundle and measure the similarity of two fiber bundles. Then we present a novel framework to optimize the shape of ROIs by maximizing fiber bundles similarity cross subjects and predict brain network ROIs in individual brain based only on DTI data. Our experimental results show that optimized ROIs have significantly improved consistency in structural profiles across subjects and demonstrated that fiber bundle description model derived from DTI data is a good predictor of functional ROIs. This capability of accurately predicting brain network ROIs would open up many applications in brain imaging that rely on identification of functional ROIs.

**Keywords:** fMRI, DTI, structural connectivity, shape optimization, ROI prediction.

## 1 Introduction

It is widely believed that the brain's function is integrated via structural and functional connectivities [1-3]. Construction of brain networks based on vivo brain imaging data offers an exciting and unique opportunity to understand cortical architecture. In brain networks, network nodes ROIs provide the structural substrates for connectivity measurement within individual brains and for pooling data across populations [2]. Therefore, a fundamental question in constructing structural and functional network is how to define the best possible regions of interests (ROIs). In our view, this task is challenging for several critical reasons. 1) The boundaries between cortical regions are unclear. 2) Individual variability of cortical anatomy, connection, and function is remarkable. Quantitative mapping of the regularity, while accounting for the variability, of cortical structure and function is a challenging task. 3) The properties of ROIs are highly nonlinear [4, 5].

Current approaches to identify ROIs can be broadly classified into four categories [6, 7]. The first is manual labeling by experts using their domain knowledge. The second is a data-driven clustering of ROIs from the brain image itself. The third is to

J. Yang, F. Fang, and C. Sun (Eds.): IScIDE 2012, LNCS 7751, pp. 390–397, 2013.
© Springer-Verlag Berlin Heidelberg 2013

predefine ROIs in a template brain, and warp them back to the individual space using image registration. Lastly, ROIs can be defined from the activated regions observed from an activation map.

Identifying ROIs using an activation map is regarded as the standard framework for ROI identification [8]. The most common approach in this framework is to create small ROIs (usually spheres) at local maxima in the activation map. Our rationale is that the activation peaks are close to the true functional ROIs, but the accuracy of their sizes and shape is dependent on several factors such as the spatial normalization procedure and individual diversity. Therefore, in this paper, we present a novel framework to optimize the shape of ROIs based on maximizing fiber bundles similarity cross subjects. In particular, we focus on optimizing the shape of default mode network ROIs using rest state fMRI (rsfMRI) data.

Additionally, the human brain is composed of many functional networks, such as default model, working memory, vision, auditory and emotion systems. Extensive acquisition of fMRI data for all these networks is both time consuming and expensive, which makes it impractical for wide use. Instead, a typical DTI images scan needs less than 10 min, is much less demanding, and is widely available. Those reasons strongly encourage us to identify and predict functionally meaningful ROIs based only on DTI data. The close relationship between structural connectivity pattern and brain function has been reported in the literature [9, 10]. An interesting observation from our recent results in [7] is that white matter (WM) fiber connection patterns of the same functional cortical ROI are reasonably consistent across different subjects, suggesting that fiber connection pattern might be a good predictor of functional ROI. Hence, in this paper, as a sequel to ROIs optimization procedure, we use the locations, shape and fiber bundles of optimized functional ROIs as the prior knowledge, and propose a new model to predict functional ROIs based only on DTI data.

The arrangement for the rest of the paper is as follows. In section 2, we firstly detail the data acquisition and preprocessing of the multimodal data including fMRI and DTI data; then, we present the fiber bundles description model and similarity measurement method; lastly, we formulate the energy function for ROI optimization and prediction. Section 3 presents some experiment results and their interpretations. Discussions and conclusion are provided in section 4.

## 2 Materials and Methods

### 2.1 Overview of the Framework

The pipeline of our framework is composed of three stages. The first stage is rsfMRI and DTI data preprocessing including independent component analysis, default mode network activation map selection and DTI tractography. The second one is group-wise optimization: after pre-processing of DTI and rsfMRI dada, rsfMRI default mode network activation map and white matter fibers were used to optimize the shape of default mode network ROIs. The third stage is prediction: given DTI data of a new subject, we predict default mode network ROIs of this subject by proposed functional ROIs prediction mode.

### 2.2 Data Acquisition and Preprocessing Method

Seven university students were recruited to participate in this study. Subjects were instructed simply to keep their eyes closed and not to think of anything in particular while fMRI data was acquired. DTI scans were also acquired for each participant. FMRI and DTI scans were acquired on a 3T GE Signa HDx scanner. Acquisition parameters were as follows, fMRI: 128x128 matrix, 2mm slice thickness, 256mm FOV, 60 slices, TR=1.5s, TE=25ms, ASSET=2; DTI: 128x128 matrix, 2mm slice thickness, 256mm FOV, 60 slices, TR=15.1s, TE= variable, ASSET=2, 3 B0 images, 30 optimized gradient directions, b-value=1000.

The following steps were done on rsfMRI data we acquired.

**Independent Component Analysis (ICA).** For each subject, after pre-processing (including brain skull removal, motion correction, spatial smoothing, temporal pre-whitening, slice time correction, global drift removal, and band pass filtering (0.01Hz~0.1Hz)),the 4D rsfMRI data was then analyzed with FSL MELODIC ICA software (http://www.fmrib.ox.ac.uk/fsl/melodic/index.html). ICA is a statistical technique that separates a set of signals into independent uncorrelated and no-Gaussian spatiotemporal components [11]. In this paper we used the default settings of MELODIC to automatically estimate the number of components from the data. And in the experiment, the number of components ranged from 29 to 35.

**Selection of the Best-Fit Component.** We select the component in each subject that most closely matched the default mode network by experts using their domain knowledge.

DTI pre-processing consisted of skull removal, motion correction, and eddy current correction. After the pre-processing, fiber tracking was performed using MEDINRIA (http://www-sop.inria.fr/asclepios/software/MedINRIA/). Fibers were extended along their tangent directions to reach into the gray matter when necessary. Brain tissue segmentation was conducted on DTI data by the method in [12] and the cortical surface was reconstructed from the tissue maps using the marching cubes algorithm. The cortical surface was parcellated into anatomical regions using the HAMMER tool [13]. DTI space was used as the standard space from which to generate the GM (gray matter) segmentation and report the ROI locations on the cortical surface. Co-registration between DTI and fMRI data was performed using FSL FLIRT [14].

### 2.3 Bundle Description Based on Gradient-Spherical Surface Mapping Model

Many algorithms, such as the spectral clustering, normalized cut clustering and atlas-based clustering, have been developed to cluster white matter fibers into different bundles. However, an open problem remains: how can a fiber bundle be described quantitatively? In this paper, we proposed a novel method called Gradient-Spherical Surface Mapping (GSSM) model to describe fiber bundle quantitatively and measure similarity of two fiber bundles.

Consider one fiber bundle $F = \{f_i, i = 1, 2, \cdots, T\}$, $T$ is the number of fibers in the bundle, $f_i$ is the *i*-th fiber which is composed of a collection of space points, denoted

by $f_i = (X_1, X_2, \cdots, X_N)$, $X_j$ is the 3D coordinate of *j*-th point, $N$ is the number of points. We define $N-1$ unit gradient directions of $f_i$ as follows:

$$\Psi_i = \left\{ g_j = \frac{X_{j+1} - X_j}{\| X_{j+1} - X_j \|_2}, j = 1, 2, \cdots, N-1 \right\} \tag{1}$$

We can see that $\| g_i \|_2 = 1$ and $g_i$ is a point in the unit spherical surface. We perform the same procedure on all fibers in the bundle $F$, and define **gradient-map** of fiber bundle $F$ as:

$$G(F) = \{ \Psi_i, i = 1, 2, \cdots T \} \tag{2}$$

Two issues should be noted here. First one is that we must make sure all subjects' brains are aligned. In this paper, we align different brains by the principal direction which is calculated using PCA. The second issue is that we need to explicitly assign one of two ends of every fiber in each fiber bundles as the starting point. Since each fiber was extracted from a small region in the brain, we select the end that is closer to the center of the region as the starting point.

After representation of fiber bundles by GSSM model, two bundles can be compared by calculating the similarity between the distributions of respective gradient-map.

As we know, unit spherical surface can be described by the following equation:

$$\begin{cases} x = \sin\alpha\cos\beta \\ y = \sin\alpha\sin\beta \\ z = \cos\alpha \end{cases} \qquad \alpha \in [0, \pi], \beta \in [0, 2\pi] \tag{3}$$

Given a positive integer $M$, unit spherical surface can be divided into $2M^2$ sub-surfaces by:

$$S_{ij} = \left\{ \begin{cases} x = \sin\alpha\cos\beta \\ y = \sin\alpha\sin\beta \\ z = \cos\alpha \end{cases} \quad \alpha \in \left[ \frac{i-1}{M}\pi, \frac{i}{M}\pi \right], \beta \in \left[ \frac{j-1}{M}\pi, \frac{j}{M}\pi \right] \right\} \tag{4}$$

$$i = 1, 2, \cdots, M, \; j = 1, 2, \cdots, 2M$$

Given gradient-map $G$, we calculate the point density of sub-surface $S_{ij}$, denoted by $\rho_G(S_{ij})$, as follows:

$$\rho_G(S_{ij}) = n_{ij} / |G| \tag{5}$$

where $n_{ij}$ is the number of points located in $S_{ij}$ and $|G|$ is total number of points in the gradient-map. Fig. 2 (e) show point density distribution of fiber bundles in Fig. 2(a), here $M = 12$, and each $\rho_G(S_{ij})$ is rearranged into a vector. The similarity of two gradient-maps $G_1$ and $G_2$ is defined as

$$D(G_1, G_2) = \sum_{i=1}^{M} \sum_{j=1}^{2M} | \rho_{G_1}(S_{ij}) - \rho_{G_2}(S_{ij}) | \tag{6}$$

Note that the point density $\rho_G(\bullet)$ is normalized so that we do not require that the numbers of points in different trace-maps are equal.

### 2.4 Optimization of ROIs across Subjects

In the data preprocessing stage, we selected default model network activation map manually in each subject. To construct default model network ROIs using those activation maps, one approach that has often been used is to threshold the activation map and construct network node ROI by activated voxels. However, this approach can be very sensitive to the specific threshold. Can we optimize the shape of ROIs by select optimal thresholds? In this section, we optimize the shape of ROIs by selecting group-wise optimal thresholds through maximize the similarity of the fiber bundles across subject and formulate the problem of optimization ROI shape as an energy minimization problem.

Taking ROI *i* for example, given a threshold $\lambda_j$ and default mode network activity map, we define $R_i^j(\lambda_j)$ as the local activated region (activation value great than $\lambda_j$) centered at location of ROI *i* on subject *j*'s surface, and fiber bundle penetrating $R_i^j(\lambda_j)$ was extracted and denoted as $f_i^j(\lambda_j)$. Then, mathematically, the energy function to minimize is defined as:

$$\left(\tilde{\lambda}_1, \tilde{\lambda}_2, \cdots, \tilde{\lambda}_p\right) = \arg\min_{\lambda_1, \lambda_2, \cdots, \lambda_p} \sum_{m=1}^{p} \sum_{n=m+1}^{p} D\left(G\left(f_i^m(\lambda_m)\right), G\left(f_i^n(\lambda_n)\right)\right) \tag{7}$$

Where $p$ is number of subjects, $G\left(f_i^m(\lambda_m)\right)$ is the gradient-map of fiber bundle $f_i^m(\lambda_m)$. By solving problem (7), we can find the optimal threshold $\left(\tilde{\lambda}_1, \tilde{\lambda}_2, \cdots, \tilde{\lambda}_p\right)$ and corresponding optimal ROIs $R_i^1\left(\tilde{\lambda}_1\right), R_i^2\left(\tilde{\lambda}_2\right), \cdots, R_i^p\left(\tilde{\lambda}_p\right)$.

### 2.5 ROIs Prediction

If the shape of fiber bundles of ROIs are descriptive enough and consistent across different brains, they can be used as good morphological signatures to predict functional ROIs in the absence of fMRI data. Therefore, an ROI prediction frame work is developed based on group-wise fiber bundles characteristics. After group-wise ROIs optimization in section 2.5, optimal ROIs and corresponding fiber bundles (we called it reference ROIs and reference fiber bundles) are used to prediction the localization and size of ROIs of a new subject (we called it target subject). Here we use a ball to describe a ROI, and average size (number of voxels) of reference ROIs is taken as the size of ball.

Suppose there are *q* reference subject, reference fiber bundles of ROI *i* denoted as $f_i^1, f_i^2, \cdots, f_i^q$, we formulated prediction progress as following energy function minimization problem:

$$\tilde{B}(x, y, z) = \arg\min_{x,y,z} \sum_{j=1}^{q} D\left(G\left(f_i^j\right), G\left(f_{B(x,y,z)}\right)\right) \tag{8}$$

where $G\left(f_i^j\right)$ is the gradient-map of fiber bundle $f_i^j$, $f_{B(x,y,z)}$ is the fiber bundle of ball $B(x,y,z)$, $(x,y,z)$ is the center of the ball, $G\left(f_{B(x,y,z)}\right)$ is the gradient-map of fiber bundle $f_{B(x,y,z)}$.

In our implementation, we first align all reference ROIs to DTI space of target subject; then calculate the center of each reference ROI to form a search space; at last, we find the solution of question (8) by whole space searching.

## 3 Experimental Results

In this section, we present some experimental results. Our results consist of 2 parts. First, we test our default mode network ROI optimization framework using dataset described in section 2.1, and show optimized ROIs and corresponding fiber bundles in section 3.1. Second, we performed leave-one-out prediction experiments and show the prediction results and some quantitative measurements in section 3.2.

### 3.1 Optimization Results of 7 Subjects and 8 ROIs

Fig 4 shows the optimized default mode network ROIs and corresponding fiber bundles of 7 subjects after optimization. From the figure it can be seen that optimized ROIs from different subjects have consistent structural connectivity profiles.

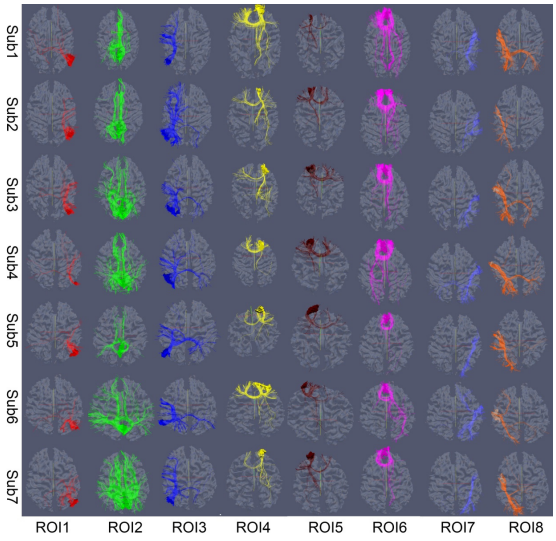


**Fig. 1.** Visualization of optimized ROIs and corresponding fiber bundles of 7 subjects

### 3.2 Leave-One-Out Prediction

We used the leave-one-out strategy to evaluate the ROI prediction framework on the dataset described in section 2.1. To visualize the consistency of fiber bundles of the predicted ROIs, we showed the fibers emanating from predicted ROIs in Fig 5.

It is evident that the fiber bundles of the predicted ROIs are quite similar to those of optimized ROIs which are shown in Fig 4.

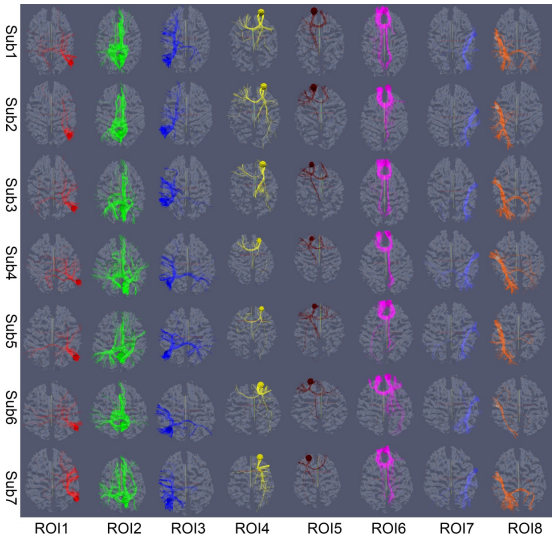


**Fig. 2.** Visualization of predicted ROIs and corresponding fiber bundles

In order to further evaluate the performance of our prediction framework, we show the Euclidean distances between centers of optimized and predicted ROIs in Table 1. We can see that most of the prediction errors are approximately 2--6 mm, which is 1--3 voxels in DTI volumes. On average, the average prediction error for ROIs is 5.5078, which is considered as very accurate.

**Table 1.** Euclidean distances between centers of optimized and predicted ROIs

| (mm) | **ROI 1** | **ROI 2** | **ROI 3** | **ROI 4** | **ROI 5** | **ROI 6** | **ROI 7** | **ROI 8** | **mean** |
|---|---|---|---|---|---|---|---|---|---|
| **sub 1** | 2.9986 | 4.6785 | 4.0883 | 5.8943 | 6.3434 | 4.2054 | 4.6815 | 1.8549 | 4.3431 |
| **sub 2** | 3.0651 | 3.9306 | 10.670 | 2.8391 | 3.6169 | 5.5907 | 5.4525 | 4.4219 | 4.9484 |
| **sub 3** | 5.5276 | 6.486 | 10.982 | 1.902 | 5.4555 | 5.7313 | 4.4985 | 6.1455 | 5.8411 |
| **sub 4** | 6.2541 | 4.8263 | 3.4572 | 4.3281 | 4.7349 | 7.8706 | 2.2865 | 6.5534 | 5.0389 |
| **sub 5** | 1.9175 | 2.4672 | 3.0958 | 13.309 | 4.1456 | 6.9007 | 9.1755 | 3.1937 | 5.5257 |
| **sub 6** | 9.0583 | 5.5533 | 14.688 | 2.6011 | 9.1592 | 14.040 | 7.1509 | 4.7839 | 8.3795 |
| **sub 7** | 5.0527 | 2.6292 | 4.3583 | 8.4163 | 0.5767 | 2.9615 | 7.6921 | 4.1348 | 4.4777 |
| **mean** | 4.8391 | 4.3673 | 7.3345 | 5.6129 | 4.8617 | 6.7573 | 5.8482 | 4.4412 | 5.5078 |

## 4 Conclusion

In this paper, we presented a novel framework for functional brain network ROI optimization and prediction using rsfMRI data and DTI data. This framework has been extensively evaluated on 8 ROIs across 7 subjects. Our optimization results indicated that the structural connectivity patterns of each individual's functional ROI are very consistent after optimization, and prediction results demonstrated that our fiber bundle description model of functional brain ROIs have remarkable prediction capability. In the future, we plan to apply and evaluate this ROI prediction framework in other brain networks, such as working memory, attention and semantics memory systems and validate this framework on clinical data sets such as the DTI data sets of Alzheimer's disease and Autism.

## References

1. Bharat, B.B., et al.: Toward discovery science of human brain function. Proc. Natl. Acad. Sci. 107(10), 4734–4739 (2010)
2. Dijk, K.R.A.V., Hedden, T., Venkataraman, A., Evans, K.C., Lazar, S.W., Buckner, R.L.: Intrinsic functional connectivity as a tool for human connectomics: theory, properties, and optimization. J. Neurophysiol. 103(1), 297–321 (2010)
3. Hagmann, P., et al.: MR connectomics: Principles and challenges. J. Neurosci. Methods 194(1), 34–45 (2010)
4. Zhang, T., Guo, L., Li, K., Jing, C., Yin, Y., Zhu, D., Cui, Z., Li, L., Liu, T.: Predicting functional cortical ROIs via DTI-derived fiber shape models. Cereb. Cortex (2011)
5. Zhu, D., Li, K., Faraco, C., Deng, F., Zhang, D., Jiang, X., Chen, H., Guo, L., Miller, S., Liu, T.: Optimization of functional brain ROIs via maximization of consistency of structural connectivity profiles. NeuroImage 55(2), 1382–1393 (2012)
6. Liu, T.: A few thoughts on brain ROIs. Brain Imaging and Behavior 5(3), 189–202 (2011)
7. Li, K., Guo, L., Zhu, D., Hu, X., Han, J., Liu, T.: Individualized ROI Optimization via Maximization of Group-wise Consistency of Structural and Functional Profiles. Neuroinformatics 10(3), 225–242 (2012)
8. Poldrack, R.A.: Region of interest analysis for fMRI. Soc. Cogn. Affect. Neurosci. 2(1), 67–70 (2007)
9. Passingham, R.E., Stephan, K.E., Kötter, R.: The anatomical basis of functional localization in the cortex. Nat. Rev. Neurosci. 3, 606–616 (2002)
10. Honey, C.J., Sporns, O., Cammoun, L., Gigandet, X., Thiran, J.P., Meuli, R., Hagmann, P.: Predicting human resting-state functional connectivity from structural connectivity. Proc. Natl. Acad. Sci 106(6), 2035–2040 (2009)
11. Beckmann, C., Smith, S.: Probabilistic independent component analysis for functional magnetic resonance imaging. IEEE Trans. Med. Imag. 23(2), 137–152 (2004)
12. Liu, T., Li, H., Wong, K., Tarokh, A., Guo, L., Wong, S.T.C.: Brain Tissue Segmentation Based on DTI Data. NeuroImage 38(1), 114–123 (2007)
13. Shen, D., Davatzikos, C.: HAMMER: hierarchical attribute matching mechanism for elastic registration. IEEE Trans. Med. Imaging 21(11), 1421–1439 (2002)
14. Jenkinson, M., Bannister, P., Brady, M., Smith, S.: Improved optimization for the robust and accurate linear registration and motion correction of brain images. Neuroimage 17, 825–841 (2002)